Journal of King Saud University – Engineering Sciences xxx (xxxx) xxx

Contents lists available at ScienceDirect

Journal of King Saud University – Engineering Sciences

journal homepage: www.sciencedirect.com

Original article

Numerical modelling and optimisation of reverberation cutback for packed spheres

A.J. Otaru [a,*,1], Z. Manko [a], O.E. Odumu [a], A.G. Isah [a], M.R. Corfield [b]

[a] Department of Chemical Engineering, Federal University of Technology, P.M.B. 065, Gidan-Kwanu Campus, Bida Road, Minna, Niger State, Nigeria
[b] Department of Electrical & Electronic Engineering, The University of Nottingham, Nottingham NG7 2RD, United Kingdom

ARTICLE INFO

Article history:
Received 30 December 2020
Accepted 7 August 2021
Available online xxxx

Keywords:
Packed spheres
Sound absorption
Modelling & optimisation

ABSTRACT

Against multiple sources of experimentally measured data, Attenborough's acoustic porous media has proven to be a better predictor of the reverberation cutback for packed beds of near-spherical structures compared to several other equivalent fluid models. Numerical predictions using Attenborough's model were therefore used to illuminate the importance of key pore-structure related parameters of packed structures on their normal incidence sound absorption spectra. A parametric study was instigated to account for the influence of void fraction and particle size on predicted broadband sound absorption properties targeting permeability values in the range of 0.3 to $2.0\times10^{-09}m^2$. This approach could assist material manufacturers and acoustic engineers in the design of highly efficient and timely packed structures for applications-specific to sound absorption.

1. Introduction

Porous structures are widely used as soundproofing and as vibration control devices. Professionals in the field of environmental noise pollution and public health have legislated for the wider application of porous materials in reducing indoor and outdoor noise pollution (Voronina and Horoshenkov, 2003). Typical examples of these porous soundproofing materials are natural fibres (wool, hemp, cotton, fur and felt (Kino and Ueno, 2008)), synthetic fibres (polyester, polyurethane, kevlar and melamine (Jorges and Malcom, 2010; Otaru, 2019a), porous metallic/ceramic structures (Otaru, 2019a; Hinze and Rosler, 2014; Li et al., 2014; Otaru, 2019b, Otaru et al., 2018; Chevillotte et al., 2010; Caniato et al., 2020) and packed structures (Dung et al., 2019; Attenborough, 1983, Voronina and Horoshenkov, 2004; Kumar et al., 2006; Horoshenkov and Swift, 2001; Hamad 2015; Eyo, 2020). The use of these materials in either their naturally occurring or synthetic forms have proven useful in reverberation cutback. However, acoustic engineers are continuously engaged in improving the overall performance of soundproofing materials; such as those used in sports halls, auditoriums, places of worship, factory spaces, designs for car catalytic converters (car mufflers) and aerospace technologies; to the reflection of sound by ground surfaces and studies of acoustic-to-seismic coupling for the estimation of the soil characteristics of porous ground surfaces (Attenborough, 1983). Analogous research work in (Voronina and Horoshenkov, 2003; Otaru et al 2019a; Dukhan, 2013, Zieliński, 2015; Perrot et al., 2008) have examined several porous soundproofing materials for this purpose, with a significant number of authors highlighting the relative importance of packed structures.

Packed beds are mostly used as constructs that interact with fluids and heat (Oahimire and Olajuwon, 2014), however, there is an applicable use for these structures as sound-absorbing materials. Generally, the permeability (k_0) of packed or granular materials is described (Dybbs and Edwards, 1984; Otaru and Kennedy, 2019) as the most important intrinsic property of the porous media and by the Kozeny-Carman empirical relation (Eqn 1), which is expressed as a test function of the Kozeny constant (K), particle size (Dp) and void fraction (ε) of the packed structures (Carman, 1956). The accuracy of this empirical model (Eqn 1) to within experimental scatter is described in (Otaru and Kennedy, 2019) to be contingent on the exact use of the Kozeny constant (K). This constant is described in (Ergun, 1952) to vary between 4.5 and 5.1 due to the complicated pore nonuniformity of porous media. This anisotropy can be described by the tortuosity (τ) of the porous

* Corresponding author.
E-mail address: otaru_12257@yahoo.com (A.J. Otaru).
[1] ORCID No: 0000-0002-3057-4991.

Peer review under responsibility of King Saud University.

Production and hosting by Elsevier

https://doi.org/10.1016/j.jksues.2021.08.005
1018-3639/

Please cite this article as: A.J. Otaru, Z. Manko, O.E. Odumu et al., Numerical modelling and optimisation of reverberation cutback for packed spheres, Journal of King Saud University – Engineering Sciences, https://doi.org/10.1016/j.jksues.2021.08.005

medium and can vary inversely for structures of different packing densities and sizes. Based on experimentally measured permeability data, Carman (1956), Alsayed and Amjad (1996) proposed $\sqrt{2}$ as the tortuosity value for granular packed structures. The proposed tortuosity value was reportedly valid for spherical structures but can deviate significantly for complex/consolidated porous materials characterised by non-spherical packed structures with a broad size distribution. Du Plessis and Fourie (2002), Ergun (1952) assigned an analytical expression for the tortuosity of highly porous ($0.88 \leq \varepsilon \leq 0.98$) microcellular structures as a test function of open-cell porosity (ε) based on a geometrical modelling of the internal structure of the porous matrices. Their proposed model was used to determine the dynamic tortuosity of "bottleneck-type" microcellular structures in (Otaru et al 2019a; Otaru et al 2019a) – with reasonable agreement between numerically predicted and experimentally measured values of their sound absorption spectra. A analytical expression for the high frequency limit of dynamic tortuosity was proposed by Umnova et al (2000), Du Plessis and Fourie (2002) for oscillatory flow in an air-dominated stack of fixed identical rigidly packed spheres. Reasonable agreement between predicted tortuosity values, published data and numerically simulated results for tortuosity of random and simple cubic packed spheres were established. Based on a workable representative cubic cell volume, Du Plessis and Masliyah (1991), Umnova et al (2000) provided an analytical expression for the dynamic tortuosity of isotropic granular media with reasonable correlation when compared to experimental measurements. Using a local volume averaging approach, Bear and Bachmat (1990) provided a mathematical continuum framework for addressing the tortuosity of monosized packed granules. The significant deviation between their predicted values and experimental measurements led to the modification of the macroscopic tensor in their model by Ahmadi et al (2011), Bear and Bachmat (1990) thereby reducing this disparity. Based on experimental conductivity measurements for freely overlapping spheres, Weissberg (1963), Bear and Bachmat (1990) provided an analytical tortuosity model as a test function of sample porosity with strong validation through experimental measurements characterised by void fractions between 0.36 and 1.0. Their work was also validated in Barrande et al (2007), Ahmadi et al (2011) despite the assumption of overlapping spherical structures being erroneous. Table 1 presents some of the analytical tortuosity models as a test function of void fraction of porous structures available in the literature.

The packing and arrangement of granular materials has the potential to reduce total sound against variable degrees of vibrating frequencies. An understanding of the pore morphological features and pore-structure related properties (non-acoustical properties) of the porous media may provide an insight into their acoustic behaviour. Analogous research work on the application of granular media for sound absorption control used either experimentally or pore-level numerical modelling and simulation approaches to account for these non-acoustical parameters. Typical examples of these parameters are permeability (k_0), void fraction (ε), kinematic tortuosity (τ), dynamic shape factor (m), and steady flow shape (s) factor (Attenborough, 1983). Though, the two shape factors in (Attenborough, 1983) were replaced with viscous (L_V) and thermal characteristic length (L_T) to account for the visco-inertial and thermal dissipating mechanism for higher frequency applications (Horoshenkov and Swift, 2001; Johnson et al., 1987). Other non-acoustic pore-structure related parameters are static thermal tortuosity (τ_T), static thermal permeability (k_T) and static viscous tortuosity (τ_0), and are used (Otaru, 2019a; Zieliński, 2015, Pride et al., 1993) along with other parameters to account for the acoustical properties of structures characterised by non-uniform sections and possible constrictions. Proposed models using these non-acoustical properties of porous media are used for evaluating their surface acoustic impedance (Z_C), complex propagation coefficient (k) and dimensionless normal incidence absorption coefficient (A_C). These acoustic porous media models are classified into empirical (Dung et al., 2019), phenomelogical (Mikki, 1990), and semi-phenomelogical (Perrot, 2006) models. These models can be described as equivalent fluid models when used for granular media (Dung et al., 2019; Attenborough, 1983).

Comparable research work on the determination of the acoustical properties of granular materials can be traced back to the work of Attenborough (1983). This work developed acoustic porous media models to predict the complex propagation coefficient and surface acoustic impedance of rigid fibrous absorbent soil and sands, yielding acceptable agreements with experimental data. A more compelling model was developed to account for the acoustical properties of granular media based on a log-normal size distribution of tortuous slit-like pores (Attenborough, 1993). The model makes use of the Bruggemann correlation (Otaru, 2019a) linking kinematic tortuosity to void fraction ($\tau = \varepsilon^{-0.5}$) and the Kozeny-Carman equation to approximate the permeability (or flow resistivity) of the granular media. Based on a Pade' approximation approach in (Horoshenkov et al., 1998), a simpler model for predicting the sound absorption spectra of porous granular materials with some assumed pore geometry and pore size distribution close to log-normal was reported in (Horoshenkov and Swift, 2001). This approach was ascribed to give a better predictive scatter to other equivalent fluid models. Kim and Lee (2010) reported numerically predicted results for the sound absorption spectra for porous concrete using "real" and "virtually-created" packed structures. The combined effects of particle size and packing geometry on the incidence plane wave developed across air-filled beds of granular materials were reported in (Kumar et al., 2006). Their study showed the dependence of natural frequencies, acoustic attenuation, and speed of sound on the void fraction of the granular medium. An examination of the physical properties of loosely packed granular beds on their acoustic absorption spectra was reported in (Voronina and Horoshenkov, 2003) and a simple empirical relationship proposed to relate a number of measurable pore-structure related properties of the loosed beds.

Zieliński (2015) reported the determination of the non-acoustical properties of "virtual-generated" randomly packed spheres based on numerical modelling and simulation of fluid and thermal transport across workable representative cells. These non-acoustical parameters were used to account for the sound absorption spectra developed across the porous matrices with reasonable correlation to experimentally measured data. In a related work (Dung et al., 2019), wall effects and dependency of the thermal characteristic length on particle size of randomly overlaying packed beds of spheres was studied. This work investigated the capacity of several equivalent fluid models in numerically predict-

Table 1
Tabular representation of tortuosity models for porous structures substantiated in the literature.

$k_0 = \frac{D_p^2}{36K}\left\{\frac{\varepsilon^3}{(1-\varepsilon)^2}\right\}$ Alsayed and Amjad (1996), Ergun (1952), Du Plessis and Fourie (2002)	$\tau = \{2 + 2\cos\left[\frac{4\pi}{3} + \frac{1}{3}\cos^{-1}(2\varepsilon - 1)\right]\}\tau = \{1 + \frac{1-\varepsilon}{\varepsilon}\}$
$\tau = \left\{\frac{\varepsilon}{1-(1-\varepsilon)^{2/3}}\right\}$ Umnova et al (2000), Bear and Bachmat (1990)	$\tau = \left\{\sqrt{\frac{2\varepsilon}{3\left[1-1.108(1-\varepsilon)^{2/3}\right]} + \frac{1}{3}}\right\}$, $\tau = \{1 - \frac{49}{100}\ln(\varepsilon)\}$ (Ahmadi et al., 2011; Weissberg, 1963) Eq. (1)

ing the sound absorption spectra of randomly packed spheres and to further provide a range of non-acoustical properties needed for the design of highly efficient soundproofing packed structures.

2. Research approach

The approach used in this study is categorised into two stages: acquisition of pore-structure related properties using randomly packed structures, as in (Otaru and Kennedy, 2019) and numerically simulating the sound absorption spectra across macroscopically defined geometries. The study in (Otaru and Kennedy, 2019) combined discrete element modelling (DEM) and simulation of packed spheres and computational fluid dynamics (CFD) modelling and simulation to account for the pressure drop across a workable representative volume of randomly packed spheres (1, 2 and 3 mm in sizes). The CFD simulation was carried out in COMSOL Multiphysics 5.2^{TM} by resolving low velocity Navier-Stokes equation for selected boundary conditions across workable volumes – similar to 3D unit cell volumes reported in (Hassan et al., 2014). The inlet and exit sections of the 3D unit cell were bounded to velocity and zero pressure, respectively, whilst the lateral faces were considered symmetric. The void fraction (between 0.34 and 0.45) of the porous medium was achieved using a negative of the packed structures with a flow permeability determined by fitting the computed pressure-velocity data developed across the packed spheres into a Hazen-Darcy model. This range of void fraction obtained for the virtually-packed structures is in agreement with experimental analysis on the determination of the porosity of natural aggregates in (Alsayed and Amjad, 1996) – using mercury a intrusion porosimetry (MIP) technique. A Kozeny constant of 4.64 was determined by fitting permeability, void fraction and particle size into a Kozeny-Carman model in (Carman, 1956). This approach is reiterated in this study with more CFD revision across densely ($\varepsilon = 0.33$) packed spheres carried out for different particle sizes as shown in Fig. 1. Fig. 1 shows two- and three-dimensional DEM packed spheres (left) and a velocity streamline/arrow plot (right) for densely packed ($\varepsilon = 0.33$) 2 mm representative spheres. Concurrence in the values of the Kozeny-constant for these densely packed structures were found to be in keeping with equivalent data ($R^2 \geq 99$ percent) in (Otaru and Kennedy, 2019); giving an insight into the ability of the well-known Ergun relation (Ergun, 1952) to accurately predict the pressure drop behaviour for a viscous-dominated flow regime. The tortuosity of the packed spheres was determined by the application of several tortuosity models in (Du Plessis and Fourie, 2002; Umnova et al., 2000; Du Plessis and Masliyah, 1991; Ahmadi et al., 2011; Weissberg, 1963; Barrande et al., 2007) and a comparison of the resulting predicted sound absorption spectra on the measured data for granular materials available in the literature. The void fraction was determined by measuring the volume fraction of the Boolean inverted representative packed structures using a 3D advanced imaging tool (ScanIP^{TM} module of Synopsys-Simpleware). Additionally, the mean particle size was achieved by statistically measuring the average value of watershed segmentation particles of the packed structures in ScanIP.

The sound absorption spectra developed across these materials were achieved by numerical modelling and simulation of Helmholtz linear acoustic and acoustic porous media models on a three-dimensional (3D) half-tube geometry in COMSOL Multiphysics^{TM}. These acoustic porous media models are Delany Bazley-Mikki [DBM] Mikki (1990), Johnson et al. (1987), Zwikker and Kosten (1949), Wilson (1993) and Attenborough models Attenborough (1983). While the JCA and Attenborough models require five pore-structure related properties to predict the specific surface acoustic impedance and complex propagation coefficient of porous materials, the DBM model is purportedly described (Otaru, 2019a; Attenborough, 1983; Mikki, 1990) to use only permeability to fully describe the acoustical behaviour of some porous materials. The Zwikker-Kosten and Wilson models are described in (Zwikker and Kosten, 1949; Wilson, 1993) to use three pore-structure related parameters to predict the acoustical properties of porous media. An in-depth understanding of several acoustic porous media models and their importance are expounded in (Otaru, 2019a).

The 3D half-tube geometry (Fig. 2b) was created using the dimensions of a 4-microphone AFD 1200-AcoustiTube® (Otaru, 2019b; Otaru et al, 2018) which consists of a speaker source, transmission tube and specimen sections, as shown by Fig. 2a. The selected material for all the domains in the geometry, is air, at saturated temperature and pressure, while defining the porous layer domain as a function of the macroscopic parameters of the porous medium. The inlet and outlet section of the 3D half-tube geometry was set to a hard-sound boundary wall with background pressure field and incidence plane wave of 1.0 Pa (acting in all directions) applied to the source and tube domains. The sidewall of the geometry was set for periodic boundary conditions, typically, Floquent periodicity. The likely trade-off between mesh count, convergence time, and accuracy was achieved by an optimum mesh balance on a 2D geometry as shown in Fig. 2c. Free triangular mesh structures were applied to the tube and porous layer domains while mapped

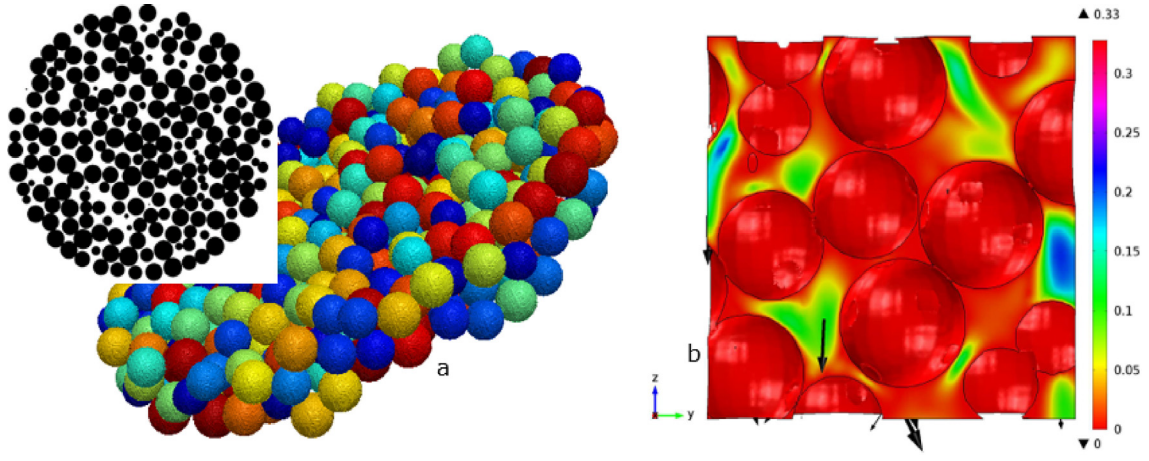

Fig. 1. (a) Left of velocity (m.s^{-1}) streamline/arrow plots of flowing fluid across representative packed spheres is a two- and three-dimensional images of virtual macroporous packed spheres characterised by particle size 2.0 mm and 0.33 void fraction.

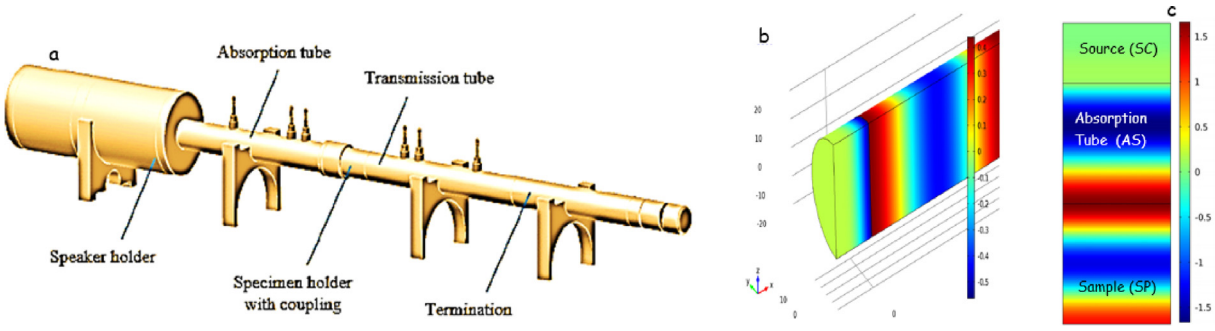

Fig. 2. (a) An AFD 1200-AcoustiTube® (adapted from (Otaru, 2019b; Otaru et al, 2018)), (b) Three-dimensional half-tube and (c) two-dimensional numerically simulated total acoustic pressure for 20 mm hardbacked packed spherical structures.

mesh structures were applied to the source domain. A minimum edge length equivalent of the minimal wavelength divided by 2000 (i.e. $c_0/2000f_{max}$, where c_0 & f_{max} are the speed of sound in air and maximum frequency limit, respectively) was used for the meshing parameter while setting the maximum element growth, curvature factor, and resolution of narrow regions to 1.3, 0.3, and 1.0 respectively. The maximum edge length in the meshing parameter section was set by varying the size between $c_0/100f_{max}$ and c_0/f_{max}. The peak value of the maximum edge length (c_0/f_{max}) yielded a very coarse mesh with cell density of 32 and significant deviation; although less is less than 50%, when compared to experimental data (Horoshenkov and Swift, 2001) for sound absorption coefficients at selected frequencies (100, 1000, 2000, and 4000 Hz). However, selected values of maximum edge length between $c_0/100f_{max}$ and c_0/f_{max} yielded a more acceptable deviation that is more than 98% in agreement with experimental data of sound absorption coefficients (Horoshenkov and Swift, 2001) for the aforementioned frequencies; resulting in cell densities between 862 and 33166. A moderate maximum edge length of $c_0/60f_{max}$ (cell density, 11750) was therefore chosen for the 2D simulation, thereby yielding negligible differences that is less than 0.05% when compared to several acoustic absorption spectra obtained on a 3D half tube simulation (cell density approximately 7.5MCells). This negligible difference in results obtained for 2D and 3D simulations can be attributed to the resolution of volume average acoustic porous media model equations that are independent of the specified domain, but rather on the representative values of the selected pore-structure related parameters provided. Hence, all numerical simulation results on sound absorption spectra were computed in 2D due to its quick convergence time and accuracy. It is noteworthy to recognise that this approach is different from a pore-scale approach where the output of the results is largely dependent on the inherent properties of a workable representative volume of the porous media (Otaru and Kennedy, 2019; Zwikker and Kosten, 1949). The normal incidence sound absorption spectra for several numerical simulations were obtained using the computed specific surface acoustic impedance (Z_c) and acoustic characteristic impedance (Z_o) of air at S.T.P., described in (Otaru 2019a; Kim and Lee, 2010). A quantitative assessment of the numerically simulated sound absorption spectra developed across several packed spheres was performed (using procedures reported in Otaru et al. (2018) with the determination of a noise reduction coefficient (NRC), sound absorption average (SAA), quarter-wavelength layer resonance peak in absorption (Ap), frequency of peak absorption (f_{peak}) and half bandwidth ($1/2f_{width}$). The average sound absorption coefficient for the twelve one-third octave band (200–2500 Hz) was determined as the SAA while the NRC was calculated as the arithmetic mean of the sound absorption coefficients for the one-third octave frequencies (250, 500, 1000 and 2000 Hz). The highest peak in absorption coefficient and variance in the frequencies at the 0.5 absorption coefficient were calculated as the Ap and $1/2f_{width}$ respectively. The results of the numerically simulated total acoustic pressure for 20 mm hardbacked packed spheres are presented in Fig. 2b and c, for both the 3D half-tube and 2D geometries, respectively.

3. Discussions of results

The accuracy of the numerical model was established by comparing the resulting predicted normal incidence absorption spectra against multiple sources of experimentally measured data available in the literature, for frequencies between 0 and 7 kHz. Fig. 3a and b present the predicted and experimentally measured (Horoshenkov and Swift, 2001) characteristic sound absorption spectra for spherical glass beads (mean particle size, 0.68 mm, and pore volume fraction, 0.38) and Coustone (mean particle size, 0.74 mm, and pore volume fraction, 0.40). Experimental values of tortuosity used for this simulation are specified in (Horoshenkov and Swift, 2001) as 1.742 and 1.664 respectively. These Figures show that DBM, Wilson, and Zwikker-Kosten models failed to reliably predict the acoustical behaviour characterised by the packed spheres. This may be attributed to the fact that these models were developed to predict the acoustical behaviour characterised by non-packed granular media. For example, work reported in (Otaru, 2019a; Otaru et al., 2019a) showed that the Wilson (1993) model is an accurate predictor of the relaxation behaviour at the boundary layer of structures characterised by spherical pores (not spherical particles) and circular openings where there is a transition in relaxation behaviour (Wilson, 1993; Otaru et al., 2019a). This geometrical description is hardly identifiable from "bottleneck-type" structures described in (Li et al., 2014; Lu et al., 2000), typified by pore-volume fractions between 0.6 and 0.8. The observed inaccuracy of the DBM model to reliably characterise the sound absorption spectra for these granular materials is also evident in Fig. 3a and b. This could be attributed to their "phenomenological focus" on high-porosity (fibrous) materials (Otaru, 2019a; Mikki, 1990). These fibrous materials are characterised as transversely isotropic in their natural state (Otaru, 2019b) with extremely high pore-volume fraction, typically, beyond 0.95%. It would, therefore, be reasonable to conclude that the predictive outcome of normal incidence sound absorption spectra using DBM models for highly porous materials would provide a better fit to experimental measurements, as evident in Fig. 3c. This figure presents numerically predicted and experimental measured (Hinze and Rosler, 2014) data of the normal incidence sound absorption spectra for highly porous metallic sponges for different porous layer thicknesses ranging from 8.0 to 17.5 mm. The experimentally measured values of permeability (reported in Hinze and Rosler,

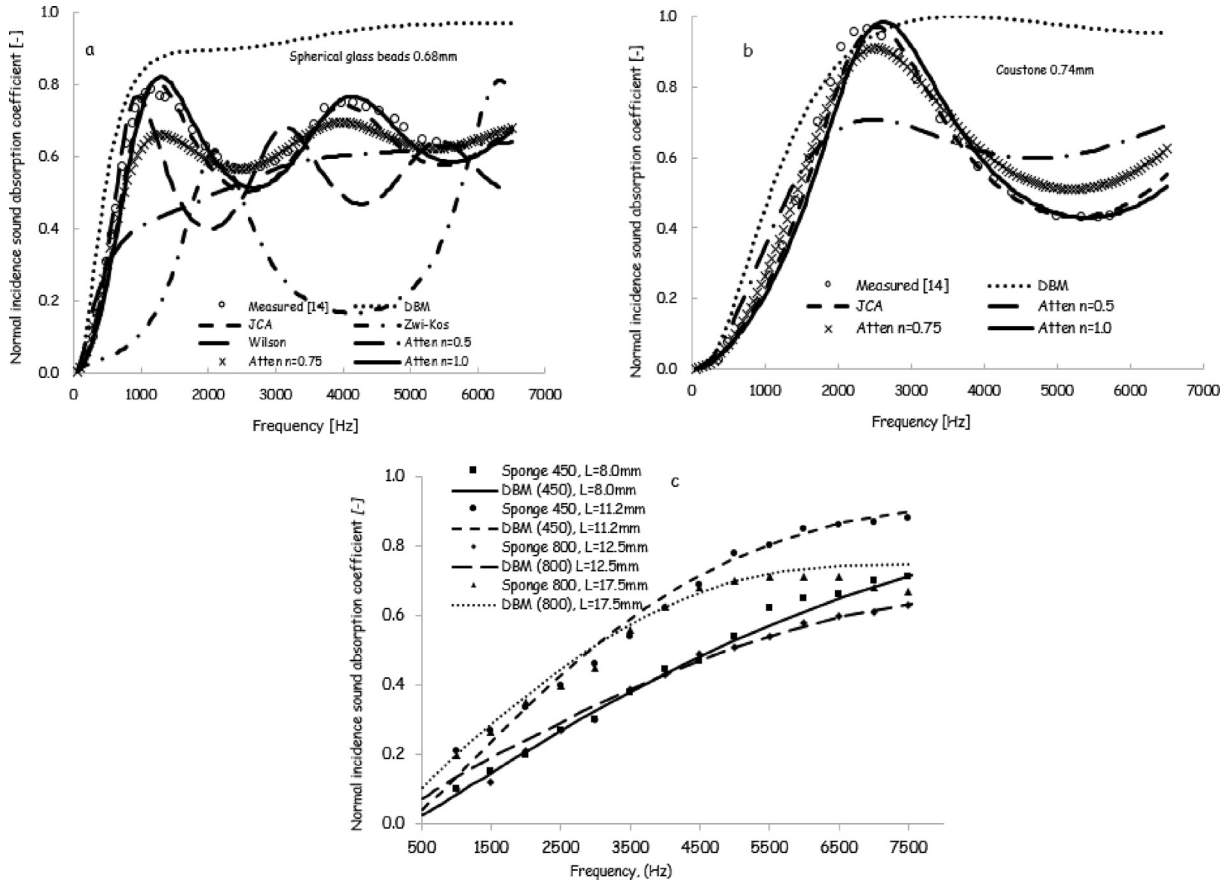

Fig. 3. Plots of dimensionless numerically simulated sound absorption spectra against multiple sources of experimentally measured data for (a) 0.68 mm size spherical beads (Horoshenkov and Swift, 2001), (b) 0.74 mm sized Coustone (Horoshenkov and Swift, 2001) and porous metallic sponges (Hinze and Rosler, 2014) for frequency (Hz).

2014) for these highly porous metallic sponges are $0.91\text{x}10^{-09}\text{m}^2$ (for the 450 sample) and $3.64\text{x}10^{-09}\text{m}^2$ (for the 800 sample) with porosities greater than 95%, for both cases; exceptionally higher than those recorded for packing beds of structures that reportedly sit between 0.33 and 0.49 pore volume fractions (Attenborough, 1983; Horoshenkov and Swift, 2001; Otaru and Kennedy, 2019; Carman, 1956).

Fig. 3a and b show that the JCA and Attenborough's model reliably predicts characteristic sound absorption spectra of the granular materials. However, the application of the JCA model requires the determination of the viscous– and thermal characteristic lengths of the granular materials using expressions reported in (Dung et al., 2019). In addition to the values of permeability, tortuosity and void fractions provided in (Horoshenkov and Swift, 2001). Predictions with the JCA model could be improved when the thermal effects are corrected using the so-called thermal permeability, that is, by means of another parameter and/or the enhanced version of JCA model, namely Johnson-Champoux-Allard-Lafarge (JCAL) model (Otaru, 2019a). The application of the Attenborough's equivalent fluid model during simulation requires the fitting of a shape factor ratio ($n = m/\sqrt{s}$). This shape factor ratio is reported in the original work of Attenborough (1983) to vary between 0.5 and 1.0 for granular media. Fig. 3a and b shows that using a shape factor ratio of 1.0, the numerically predicted normal incidence sound absorption spectra of the spherical granular materials completely overlay the experimentally measured data, better than the application of the JCA model. Though, the JCA model was originally developed to account for the acoustical behaviour of motionless skeleton structures characterised by arbitrary pore shapes (Johnson et al., 1987) and irregular pore network influenced by high pore volume fractions (between 0.8 and 0.95%), saturated by a Newtonian fluid (Chevillotte, 2010). More so, the exact use of a shape factor ratio in Attenborough's model could help in reducing the gap between predicted and measured acoustical properties for these structures, as evident in Fig. 3c. It is noteworthy to recognise that Attenborough's model (1983) was modified from the Zwikker and Kosten (1949) model developed for porous materials with elastic frames. The Attenborough's model was reportedly valid for predicting the acoustical properties of rigid fibrous absorbents and sands using five pore-structure related parameters of the porous media (permeability, pore-volume fraction, kinematic tortuosity, dynamic shape factor, and steady flow shape factor).

Experimental values of the tortuosity (as part of the pore-structure related properties) used in the numerical simulation approach in Fig. 3a and b are provided in (Horoshenkov and Swift, 2001). The influence of the changes associated with varying tortuosity of porous media is established by the application of several void-fraction-dependent tortuosity models available in the literature (Du Plessis and Fourie, 2002; Umnova et al., 2000; Du Plessis and Masliyah, 1991; Ahmadi et al., 2011; Weissberg, 1963; Barrande et al., 2007), given by Eq. (1). Fig. 4a and b show the plots of the numerically simulated normal incidence sound absorption spectra against experimental measurements (Dung et al., 2019) for 2 mm [permeability, $3.14\text{x}10^{-09}\text{m}^2$] and 5 mm [permeability, $1.75\times10^{-08}\text{m}^2$] mean particle size packed spheres, respectively. It is evident from these figures that the characteristic sound absorption spectra obtained using Weissberg (1963) tortuosity model (also reported in (Barrande et al., 2007)) completely superimpose experimentally measured data recorded in both

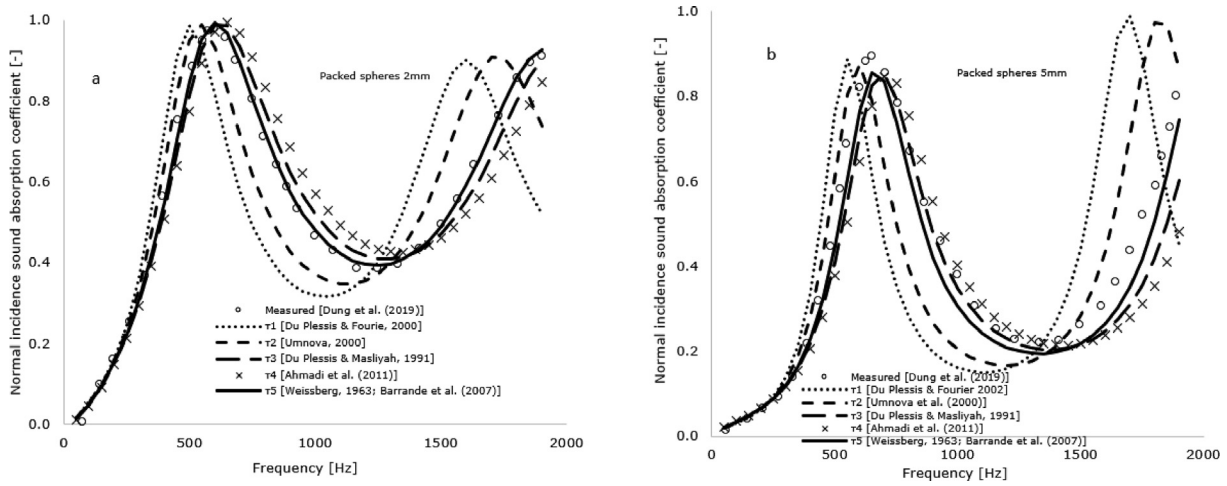

Fig. 4. Plots of the dimensionless numerically simulated normal incidence absorption coefficient using different tortuosity (τi) predictive models against experimentally measurements (Dung et al., 2019) for packed spheres characterised by (a) 2 mm and (b) 5 mm mean particle size.

cases. These equitable agreements could allude to the theory that, the Weissberg's tortuosity model was developed using experimental conductivity measurement for freely overlaying packed beds of spheres (Ahmadi et al., 2011; Barrande et al., 2007) and are highly accredited by researchers in the field of transport in porous media. The application of the Weissberg analytical model shows that the range of tortuosity values obtained for monosized packed structures used in this work varies between 1.387 (for loosely packed spheres) and 1.543 (for densely packed spheres). The constant value of $\sqrt{2}$ provided by Carman (1956) as the tortuosity for granular packed structures sits within the predicted values using the Weissberg (1963) tortuosity correlation. However, the resulting predictions of the normal incidence sound absorption spectra in Fig. 4 convey strong support to the supposition that a generalised value of the tortuosity of packed spheres is universally untrue and could lead to inaccuracies when used to evaluate the acoustical properties of near-spherical packed structures.

The potential to improve the sound absorption properties of packed spheres was studied by assessing the influence of central pore-structure related parameters of the porous media. Using Attenborough's (1983) model with a shape factor ratio of 1.0, the mean particle size (Dp) and pore volume fraction (ε) were varied within limits that would be realistically possible for packed beds, as previously reported in (Horoshenkov and Swift, 2001; Carman, 1956) to influence the permeability and tortuosity of porous media. Fig. 5a and b present the changes associated with the sound absorption spectra of packed spheres for varied particle sizes and pore volume fraction, respectively. As expected, the sound absorption spectra varies discordantly with changes to these pore-structure related parameters. The contacts between the vibrating air and the walls of the packed particles are described in (Zhang and Zhao, 2007) to dissipate a significant amount of heat energy at audible frequencies, typically, beyond 1 kHz. At lower frequencies, interparticle collision is described (Olny and Panneton, 2008; Allard and Champoux, 1992) to be elastic with little or no dissipated energy confined to large wavelengths. These figures show that the highest quarter-wavelength layer peaks in absorption (Ap) are obtained at audible frequencies, typically, between 3.0 and 4.0 kHz. This peak was reportedly (Li et al., 2014; Otaru et al., 2019a) identified to exist for frequencies between 2.0 and 3.0 kHz for "bottleneck-type" microcellular structures made by replication casting techniques. However, a significant dip in the characteristic absorption spectra beyond the 3 kHz frequency mark was observed in their work (Li et al., 2014; Otaru et al., 2019a), thereby, yielding a lesser half broadband width when compared to the packed spheres used herein. Fig. 5a and Table 2 show that the highest absorption peak (0.964) and half broadband width (2730 Hz) were observed for the 1 mm mean particle size structures – with an improved shift in absorption spectra to the frequency minima. However, lower sound absorption properties are obtained for the 3 mm packed structures and a shift in quarter wavelength layer peak in absorption to the frequency maxima is also observed. Fig. 5a also shows the sound absorption spectra for packed beds typified by mean particle size between 0.2 and 0.5 mm (smaller size packed structures) as discussed later.

Fig. 5b shows that the reduction in the pore-nonuniformity (tortuosity) of the packed bed (resulting from increasing void fraction from 0.33 to 0.43), effectively reduces their sound absorption spectra with a shift in the quarter wavelength layer peak in sound absorption to the frequency maxima. This change may be attributed to the varied pore spaces available for the propagation of pressure waves which is observably highest for the densely packed structures, typified by a pore volume fraction of 0.33, and lowest for the loosely packed structures. The negligible difference in the sound absorption spectra for these packing arrangements (Fig. 5b) at extremely high frequencies (beyond 4000 Hz) could be attributed to the unchanging wall effects exhibited by these packed structures. A measure of the specific surfaces (ratio of surface area to the volume) for the workable representative matrices (Fig. 5b) indicates a negligible difference in values observed for the different packing densities. However, differences in measured specific surfaces of the packed structures characterised by different particle sizes were significant, highest for the smallest particle size structures and lowest for the largest particle size structures. Furthermore, the numerically simulated sound absorption spectra presented in Fig. 5a and b provide an insight into the belief that densely packed structures enable the penetration of longer-wavelengths (Chevillotte, 2010) whilst differences in particle size results in the changes associated with an increase of thermal boundary layer at audible frequencies (Dung et al., 2019; Olny and Panneton, 2008).

Fig. 5a shows that the numerically predicted normal incidence sound absorption spectra for large size packed spheres are quite poor, even when approximated as densely packed. Continuous improvement of the sound absorption properties was, therefore, limited to smaller sized spheres, by studying the acoustical properties of structures characterised by 200 and 500 μm mean particle size. Fig. 5a shows that the extent to which the packed structures

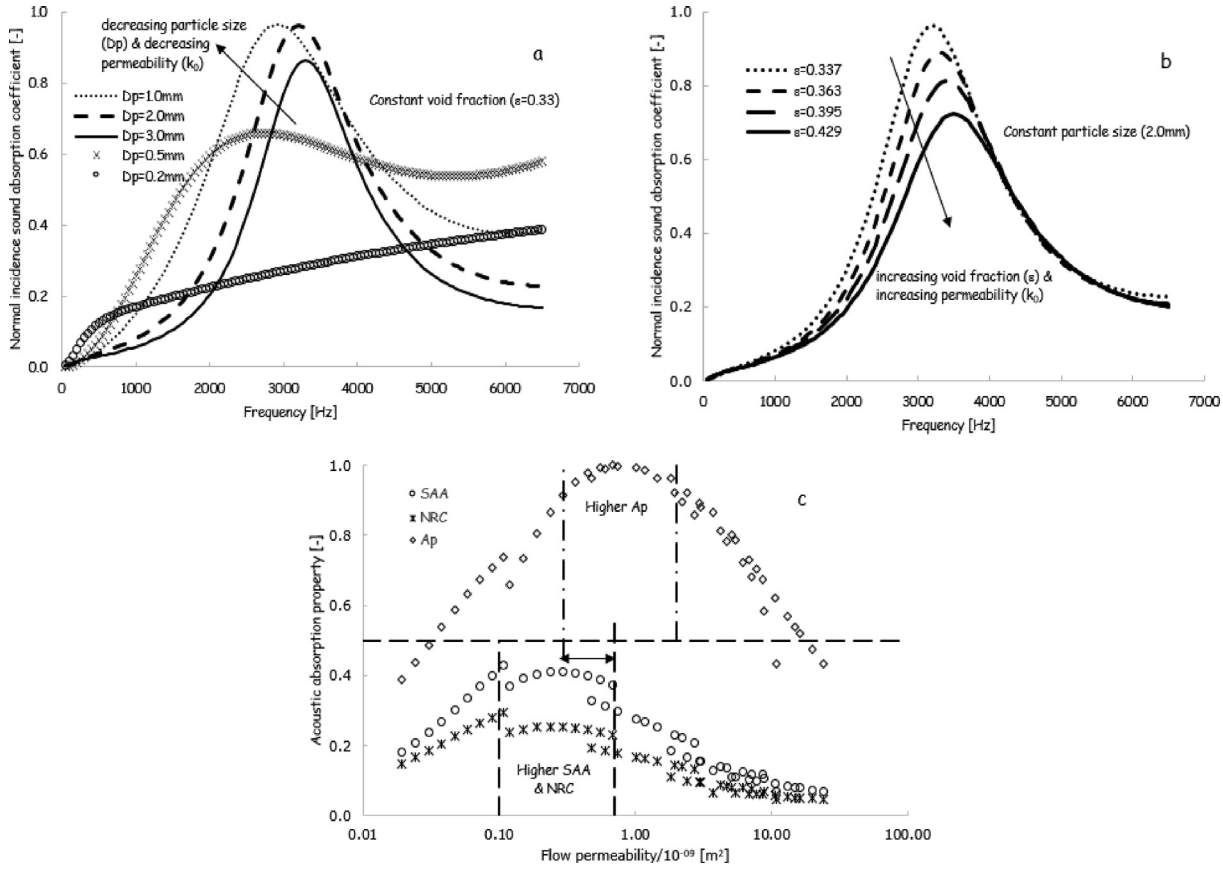

Fig. 5. Plots of the dimensionless numerically simulated normal incidence absorption coefficient for varying (a) particle size and (b) pore volume or void fraction while (c) represents plots of predicted sound absorption properties against flow permeability for particles in the range of 0.2 – 4.0 mm and void fractions between 0.33 and 0.49.

Table 2
Tabulated values of pore-structure related parameters and sound absorption properties of packed spheres.

ds (mm)	ε	$k_0/10^{-09}$ [m^2]	τ[–]	SAA [–]	NRC [–]	Ap [–]	f_{peak} [HZ]	$1/2f_{width}$ [HZ]
2.00	0.337	1.836	1.533	0.186	0.111	0.962	3200	1920
	0.363	2.938	1.497	0.156	0.095	0.890	3300	1725
	0.395	4.204	1.455	0.140	0.087	0.813	3400	1685
	0.429	6.155	1.415	0.124	0.078	0.723	3500	1500
1.00	0.33	0.476	1.543	0.326	0.194	0.964	2900	2730
3.00		3.720		0.128	0.066	0.864	3300	1500
0.50		0.120		0.370	0.236	0.660	2750	Nil
0.20		0.019		0.181	0.146	0.388	6500	Nil

thrust back pressure wave (characterised by reduced quarter-wavelength layer peak in sound absorption) were obtained for these smaller size spheres, that are densely packed ($\varepsilon = 0.33$). A significant improvement in the characteristic sound absorption properties of the packed spheres was achieved by increasing the available pore spaces of the smaller size packed structures. The combined values of their sound absorption properties (NRC, SAA, and Ap) for all packed spheres were plotted against their flow permeability values as shown by Fig. 5c. This figure indicates that improved sound absorption properties are observably high for permeability values between 0.3 and $2.0\times10^{-09}m^2$. Observations from the raw data show that this range of permeability values is attained for 500 μm loosely packed (void fractions between 0.43 and 0.49) and 1000 μm densely packed (void fractions between 0.33 and 0.37) spherical structures. A strong indication that, for varied pore volume fractions, optimum sound absorption properties of packed spheres exist in structures characterised by mean particle sizes between 500 and 1000 μm. Fig. 5c also demonstrates that, outside this range of optimal mean particle size and flow permeability values, the characteristic sound absorption properties are evidently poor and reverberation cutbacks are observably less than half for most cases.

Finally, further improvements in the characteristic sound absorption properties for the optimally selected samples were done by the insertion of an air gap (AG, also known as back cavity (Otaru, 2019a)) and increased porous layer thickness (AT) and numerically simulating their normal incidence sound absorption spectra against frequency, as shown in Fig. 6. These figures show that higher broadband noise control and a shift in the quarter wavelength layer peak in resonance absorption to the frequency minima were recorded in both cases, but, improved for the back-cavity application. This approach demonstrates the importance of back cavity application over improved porous layer thickness at lower frequencies (typically, between 0 and 2000 Hz) and in terms

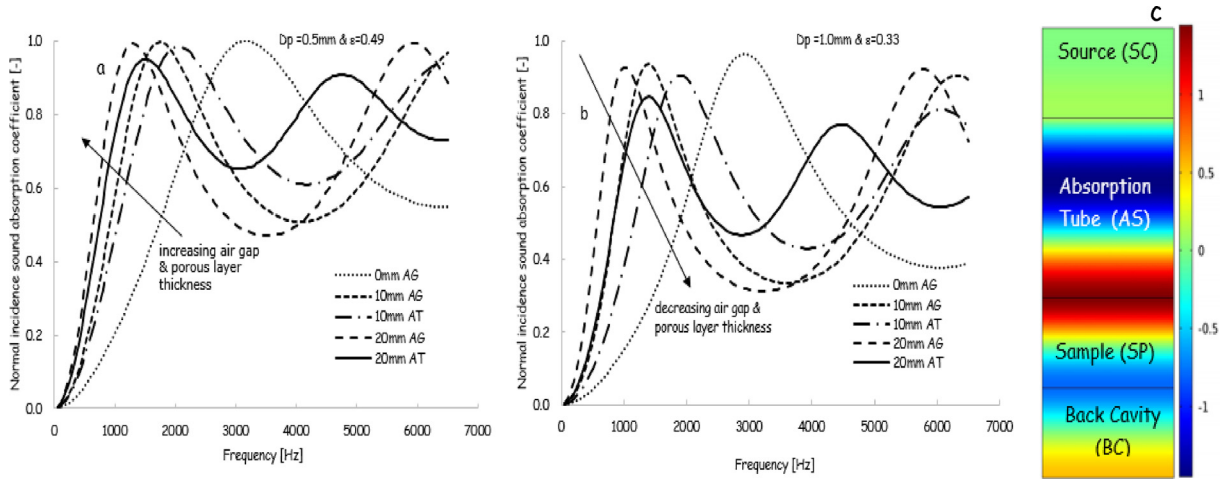

Fig. 6. Plots of dimensionless numerically simulated normal incidence sound absorption coefficient for increasing air gap (back cavity) and porous layer thickness for optimally selected pore-related parameters (a) Particle size, 0.5 mm & void fraction, 0.49 and (b) particle size, 1 mm & void fraction, 0.33. Fig. 6c. Plot of total acoustic pressure of 2D incidence plane wave on porous sample supported with an air gap or back cavity.

of cost-benefit and load-impact advantages, this approach would, therefore, be suitable for the range of the optimally selected packed spherical structures.

4. Conclusion

This work provides an insight into the propensity of Attenborough's equivalent fluid model as an accurate predictor of the characteristic sound absorption spectra typified by packed spheres and which conspicuously overlays experimental measurements when compared to other equivalent fluid models. Numerical predictions using Attenborough's model were able to demonstrate the reliability of the characteristic sound absorption spectra on the importance of pore-structure related parameters (permeability, particle size, and pore-volume fraction) of the packed spheres. Significant improvements in the characteristic sound absorption spectra coupled with a shift in the quarter wavelength layer frequency resonance absorption to frequency minima were achieved by targeting permeability values in the range between 0.3 and $2.0\times10^{-09}m^2$ and the implementation of back-cavity and increased porous layer thickness for highly efficient sound absorption. This approach could lead to desirable and timely packed structures capable of reducing noise pollution by more than half.

Declaration of Competing Interest

The authors declare that they have no known competing financial interests or personal relationships that could have appeared to influence the work reported in this paper.

Acknowledgments

Dr. AJ. would like to thank the University of Nottingham (Nottingham-UK), Petroleum Technology Development Fund (Abuja-Nigeria), Synopsys-Simpleware Ltd (California-USA), Bowers and Wilkins Group (West Sussex-UK) and Prof. Andrew R. Kennedy (Lancaster University, Lancaster-UK) for the provision of funds, licenses and technical support needed for the completion of this task.

References

Voronina, N.N., Horoshenkov, K.V., 2003. A New Empirical Model for the Acoustic Properties of Loose Granular Media. Applied Acoustics 64, 415–432.

Kino, N., Ueno, T., 2008. Comparison between Characteristic Lengths and Fiber Equivalent Diameter in Glass Fiber and Melamine Foam Materials of Similar Flow Resistivity. J. App. Acoustics 69, 325.

Jorges, P. A. & Malcom, J. C. (2010). Recent-Trends in Porous Sound-Absorbing Materials, Sound and Vibration, 44, 12-17.

Otaru, A.J. 2019a. Review on the Acoustical Properties and Characterisation Methods of Sound Absorbing Porous Structures: A focus on microcellular structures made by a replication casting method, Met. Mater. Int. DOI: https://doi.org/10.1007/s12540-019-00521-y.

Hinze, B., Rosler, J., 2014. Measuring & Simulating Acoustic Absorption of Open-Celled Metals. Advanced Engineering Materials 16. No 3.

Li, Y., Zhendong, L., Han, F., 2014. Airflow Resistance and Sound Absorption Behaviour of Open-celled Aluminium Foams with Spherical Cells. Procedia Materials Science 4, 187–190.

Otaru, A.J., 2019b. Enhancing the Sound Absorption Performance of Porous Metallic Structures using Tomography Images. Applied Acoustics 143, 183–189.

Otaru, A.J., Morvan, H.P., Kennedy, A.R., 2018. Modelling and Optimisation of Sound Absorption in Replicated Microcellular Metals. Scripta Materialia 150, 152–155.

Chevillotte, F., Perrot, C., Panneton, R., 2010. Microstructure Based Model for Sound Absorption Predictions of Perforated Closed-cell Metallic Foams. J. Acoust. Soc. Am. 128 (4), 1766–1776.

Caniato, M., D'Amore, G.K., Kaspar, J., Gasparella, A., 2020. Sound Absorption Performance of Sustainable Foam Materials: Application of Analytical and Numerical Tools for the Optimization of Forecasting Models. Applied Acoustics 161, 107166.

Dung, V.V., Panneton, R., Gagné, R., 2019. Prediction of Effective Properties and Sound Absorption of Random Close Packings of Monodisperse Spherical Particles: Multiscale Approach. J. Acoust. Soc. Am. 145 (6), 3606–3624.

Attenborough, K., 1983. Acoustical Characteristics of Rigid Fibrous Absorbents and Granular Materials. J. Acoust. Soc. Am. 73 (3), 785–799.

Voronina, V.V., Horoshenkov, K.V., 2004. Acoustic Properties of Unconsolidated Granular Mixes. Applied Acoustics 65, 673–691.

Kumar, S.T., Patle, M.K., Sujith, R.I., 2006. Characteristics of Acoustic Standing Wave in Packed-Bed Columns. AIChE Journal 53, 297–304.

Horoshenkov, K.V., Swift, M.J., 2001. The Acoustic Properties of Granular Materials with Pore Size Distribution Close to Log-Normal. Acoustical Society of America 110 (5), 2371–2378.

Hamad, A.J., 2015. Size and Shape Effects of Specimen on the Compressive Strength of HPLWFC Reinforced with Glass Fibres, Journal of King Saud University –. Engineering Sciences 29 (4), 373–380.

Eyo, E.U., Ng' ambi, S. & Abbey, S.J. (2020). An Overview of Soil – Water Characteristic Curves of Stabilised Soils and their Influential Factors, Journal of King Saud University – Engineering Sciences, doi.org/10.1016/j.jksues.2020.07.013

Dukhan, N., 2013. Metal Foams: Fundamental and Applications. DESTECH Publication, Inc., Technology & Engineering USA, 1–310.

Zieliński, T.G., 2015. Generation of Random Microstructures and Prediction of Sound Velocity and Absorption for Open Foams with Spherical Pores. J. Acoust. Soc. Am. 137 (4), 1790–1801.

Perrot, C., Chevillotte, F., Panneton, R., 2008. Bottom-up Approach for Microstructure Optimisation of Sound Absorbing Materials. J. Acoust. Soc. Am. 124 (2), 940–948.

Oahimire, J.I., Olajuwon, B.I., 2014. Effect of Hall Current and Thermal Radiation on Heat and Mass transfer of a Chemically Reacting MHD Flow of a Micropolar Fluid through a Porous Medium, Journal of King Saud University –. Engineering Sciences 26 (2), 112–121.

A. Dybbs, R.V. Edwards. 1984. A New Look at Porous Media Fluid Mechanics-Darcy to Turbulent, inJ. Bear, M.Y. Nato ASI series E.

Otaru, A.J. & Kennedy, A.R. (2019). Investigation of the Pressure Drop across Packed Beds of Spherical Beads: Comparison of empirical models with pore-level computational fluid dynamics simulations, ASME Fluids Eng'g., Vol. 141/ 071305-1.

Alsayed, S.H., Amjad, M.A., 1996. Strength, Water Absorption and Porosity of Concrete Incorporating Natural and Crushed Aggregate, Journal of King Saud University –. Engineering Sciences 8 (1), 109–119.

Carman, P.C. (1956). Fluid Flow through Granular Beds, Chemical Engineering Research & Design: Transactions of the Institution of Chemical Engineers, Part A, 15, 415-421.

Ergun, S., 1952. Fluid Flow through Packed Columns. Chemical Engineering Progress 48, 89–94.

Fourie, J.G., Du Plessis, J.P., 2002. Pressure Drop Modelling in Cellular Metallic Foams. Chem. Eng. Sci. 57 (14), 2781–2789.

Umnova, O., Attenborough, K., Li, K.M., 2000. Cell Model Calculations of Dynamic Drag Parameters in Packing of Spheres. J. Acoust. Soc. Am 107, 3113–3119.

Du Plessis, J.P., Masliyah, J.H., 1991. Flow through Isotropic Granular Porous Media. Transport in Porous Media 6, P207.

Bear, J., Bachmat, Y., 1990. Introduction to Modeling of Transport Phenomena in Porous Media. Kluwer Academic, Dordrecht.

Ahmadi, M.M., Mohammadi, S., Hayati, A.N., 2011. Analytical Derivation of Tortuosity and Permeability of Monosized Spheres: A Volume Averaging Approach. Physics Review E 83, 026312.

Weissberg, H.L., 1963. Effective Diffusion Coefficients in Porous Media. J. Appl. Phys. 34, 297–303.

Barrande, M., Bouchet, R., Denoyel, R., 2007. Tortuosity of Porous Particles. Anal. Chem. 79, 9115–9121.

Johnson, D.L., Koplik, J., Dashen, R., 1987. Theory of Dynamic Permeability & Tortuosity in Fluid-Saturated Porous Media. J. Fluid Mech. 176, 176–402.

Pride, S.R., Morgan, F.D., Gangi, A.F., 1993. Drag Forces of Porous-Medium Acoustics. Phys. Rev. B. 47 (9), 4964–4978.

Mikki, Y., 1990. Acoustical Properties of Porous Materials-Modifications of Delany Bazley Model. J. *Acoust. Soc., Jpn* (E) 11 (1), 19–24.

Perrot, C., 2006. Microstructure & Acoustic Macro-Behaviour: Approach by Reconstruction of a Representative Elementary Cell Ph.D. Thesis. University of Sherbrooke, Quebec, Canada.

Attenborough, K., 1993. Models for the Acoustical Properties of Air-Saturated Granular Media. Acta Acust. 1, 213–226.

Horoshenkov, K.V., Attenborough, K., Chandler-Wilde, S.N., 1998. Pade Approximation for the Acoustical Properties of Rigid Frame Porous Media with Pore Size Distribution. J. Acoust. Soc. Am. 104, 1198–1209.

Kim, H.K., Lee, H.K., 2010. Acoustic Absorption Modelling of Porous Concrete Considering the Gradation and Shape of Aggregates and Void ratio. Journal of Sound and Vibration 329, 866–879.

Hassan, M.I., Hassan, H.M., Abid, G.A., 2014. Study of the Axial Heat Conduction in Parallel Flow Microchannel Heat Exchanger. Journal of King Saud University – Engineering Sciences 26 (2), 122–131.

Zwikker, C., Kosten, C.W., 1949. Sound Absorbing Materials. Elsevier, New York.

Wilson, K., 1993. Relaxation-Matched Modelling of Propagation through Porous Media, Including Fractal Pore Structure. J. Acoust. Soc. Am. 94 (2), 1136–1145.

Otaru, A.J., Morvan, H.P., Kennedy, A.R., 2019a. Numerical Modelling of the Sound Absorption Spectra for Bottleneck Dominated Porous Metallic Structures. Applied Acoustics 151, 164–171.

Lu, T.J., Chen, F., He, D., 2000. Sound Absorption of Cellular Metals with Semi-Open Cells. J. Acoust. Soc. Am. 108 (4), 1697–1709.

Otaru, A.J., Morvan, H.P., Kennedy, A.R., 2019b. Airflow Measurement across Negatively-Infiltration Processed Porous Aluminium Structures. American Institute of Chemical Engineers, AIChE J. 65, 1355–1364.

Zhang, L. P. & Zhao, Y. Y. (2007). Fabrication of High-Melting-Point Porous Metals by Lost Carbonate Sintering, Proceedings of the Institution of Mechanical Engineers Part B Journal of Engineering Manufacture, 222(2), 267-271.

Olny, X., Panneton, R., 2008. Acoustic Determination of the Parameters Governing Thermal Dissipation in Porous Media. J. Acoust. Soc. Am. 123, 814–824.

Allard, J.-F., Champoux, Y., 1992. New Empirical Equations for Sound Propagation in Rigid Frame Fibrous Materials. J. Acoust. Soc. Am. 91 (6), 3346–3353.